First results of the use of a continuously flowing lithium limiter in high performance discharges in the EAST device

2016 Nucl. Fusion 56 046011

(http://iopscience.iop.org/0029-5515/56/4/046011)

IOP Publishing | International Atomic Energy Agency Nuclear Fusion

Nucl. Fusion **56** (2016) 046011 (14pp) doi:10.1088/0029-5515/56/4/046011

First results of the use of a continuously flowing lithium limiter in high performance discharges in the EAST device

J.S. Hu[1], G.Z. Zuo[1], J. Ren[1], Q.X. Yang[1], Z.X. Chen[1], H. Xu[1], L.E. Zakharov[2], R. Maingi[3], C. Gentile[3], X.C. Meng[1,4], Z. Sun[1], W. Xu[1], Y. Chen[1], D. Fan[1], N. Yan[1], Y.M. Duan[1], Z.D. Yang[1], H.L. Zhao[1], Y.T. Song[1], X.D. Zhang[1], B.N. Wan[1], J.G. Li[1] and EAST Team

[1] Institue of Plasma Physics, Chinese Academy of Sciences, Hefei, Anhui 230031, People's Republic of China
[2] LiWallFusion, PO 2391, Princeton, N J 08543, USA
[3] Plasma Physics Laboratory Princeton, Princeton University, N J 08543, USA
[4] Department of Applied Physics, Hunan University, Changsha 410082, People's Republic of China

E-mail: hujs@ipp.ac.cn

Received 9 October 2015, revised 18 January 2016
Accepted for publication 12 February 2016
Published 16 March 2016

Abstract

As an alternative choice of solid plasma facing components (PFCs), flowing liquid lithium can serve as a limiter or divertor PFC and offers a self-healing surface with acceptable heat removal and good impurity control. Such a system could improve plasma performance, and therefore be attractive for future fusion devices. Recently, a continuously flowing liquid lithium (FLiLi) limiter has been successfully designed and tested in the EAST superconducting tokamak. A circulating lithium layer with a thickness of <0.1 mm and a flow rate ~2 $cm^3\ s^{-1}$ was achieved. A novel in-vessel electro-magnetic pump, working with the toroidal magnetic field of the EAST device, was reliable to control the lithium flow speed. The flowing liquid limiter was found to be fully compatible with various plasma scenarios, including high confinement mode plasmas heated by lower hybrid waves or by neutral beam injection. It was also found that the controllable lithium emission from the limiter was beneficial for the reduction of recycling and impurities, for the reduction of divertor heat flux, and in certain cases, for the improvement of plasma stored energy, which bodes well application for the use of flowing liquid lithium PFCs in future fusion devices.

Keywords: lithium, flowing liquid limiter, plasma facing material, EAST

(Some figures may appear in colour only in the online journal)

1. Introduction

Magnetic confinement fusion offers one of the most promising approaches to nuclear fusion that potentially provides an environmentally friendly and intrinsically safe energy source with an abundant fuel supply. High-performance and steady-state operation are crucial goals of current magnetic fusion research [1–3]. Although long-pulse plasma operation has been demonstrated in various fusion experiments, a great challenge facing future fusion devices is to achieve a steady-state plasma regime with acceptable divertor heat flux in future fusion devices, especially in a fusion reactor with burning plasma. At present, solid plasma-facing components (PFCs), such as carbon (C) and tungsten (W), are popular and widely investigated. However, solid PFCs have a steady-state heat flux removal limit of ~5–10 MW m^{-2} [4]. Liquid PFCs represent a potential solution to the problems of power extraction in future power-producing reactors by reducing the heating power requirements in the expected enhanced confinement regimes.

Lithium (Li) is as an excellent candidate material for liquid PFCs. It has low ionization potential, and can therefore be easily ionized in the edge plasma. In burning plasmas, Bremsstrahlung radiation intensity increases with the Z of impurities; consequently, core plasmas have a higher tolerance for Li because it is low-Z. In addition, Li can significantly decrease the other impurity levels in the plasma, and control the recycling in edge due to its high chemical activity and adsorption capacity for hydrogen species. Low edge recycling increases the edge temperature and could create a flattened temperature distribution, which should reduce turbulence driven by temperature gradients in the plasma. Reduced turbulence, the main driver of anomalous transport, increases particle and energy confinement. Thus, liquid Li PFCs can enhance plasma energy confinement, which can lead to an innovative tokamak regime with reduced heat flux from the plasma [5]. Further, liquid Li PFCs, in principle, withstand higher heat and particle fluxes than solid PFCs while protecting the underlying solid substrates by sacrificial evaporative cooling [6].

Li has exceptional particle pumping properties, and has been successfully applied as the plasma facing material in many devices. In TFTR, long energy confinement time and high *D-T* fusion power production were obtained by injection of Li pellets into plasmas [7]. Li coatings have also significantly improved the plasma performances and L-mode to H-mode power threshold by 20–30% in TJ-II [8] and in NSTX [9]. Edge Local Mode (ELM)-free periods of enhanced pedestals were obtained with Li conditioning in NSTX [10–14]. EAST, using real-time Li aerosol injection, found complete elimination of large ELMs [15]. In addition, enhanced H-mode pedestals were obtained with Li injection in DIII-D [16]. Also, low recycling, reduced impurity level, and improved confinement were achieved in CDX-U [17], FTU [18], NSTX [19] and T-11 M [20] with Li limiters of different designs. CDX-U in particular showed a four-fold confinement enhancement with liquid Li PFCs, while LTX (Lithium Tokamak eXperiment) has shown up to a ten-fold increase, including energy confinement as high as 3–4 times H-mode scaling [20]. Finally, a Li limiter with capillary-porous system (CPS) structure successfully suppressed liquid droplet ejection by disruptions, in FTU [18], NSTX [19] and T-11 M [20]. Additionally, high performance discharges obtained in LTX with liquid lithium walls suggests the importance of 'fresh' surfaces when liquid lithium is used [21]. Tritium retention is one of shortages of Li in future fusion device, which should be overcome.

The institute of plasma physics in China (ASIPP) has had a long-term program on the Li application for PFCs on two superconducting tokamaks. One device was HT-7 (shut down in 2012) and the other is the experimental advanced superconducting tokamak (EAST). EAST was built to demonstrate high-power, long-pulse operations under fusion-relevant conditions, with major radius $R = 1.9$ m, minor radius $a = 0.5$ m and design pulse length up to 1000 s [3, 22, 23]. The maximum plasma current and toroidal field currently achieved in EAST are $I_p = 1$MA and $B_T = 3.5$ T. EAST has an ITER-like D-shaped cross section with two symmetric divertors at the top and bottom, accommodating both single null (SN) and double null (DN) divertor configurations. In order to facilitate long-pulse operations, EAST undertook an extensive upgrade to replace carbon tiles on the main chamber wall by molybdenum (Mo) tiles in 2012, with enhanced baking capability over 250 °C.The first H-mode plasma was obtained in 2010 after Li coating [24], and stationary, reproducible H-modes with duration >30 s were obtained in 2012 [3]. In addition, Li granules were injected to pace small ELMs in EAST, using a simple prototype Li injector [25]. Finally, a breakthrough was made in achieving a new steady-state H-mode without the presence of large ELMs for a duration exceeding hundreds of energy confinement times, by using a novel technique of continuous real-time injection of a Li aerosol into the edge plasma [15].

The ultimate aim of the Li program at ASIPP is to realize a large-area flowing liquid Li divertor on EAST that corresponds to low recycling, high confinement concept described above. Accordingly, the objectives of the flowing liquid Li PFCs require development of the technologies of continuously flowing Li in a tokamak, while improving wall conditions for plasma operation. First, a bench test of the flowing liquid Li limiter concept has been conducted. Initial tests, many on HT-7, have resolved several of the technology issues associated with a liquid Li loop, e.g. filling and driving the Li, heating, the use of valves and Li collection techniques. Movable liquid Li limiters either with a free-surface or a CPS were successfully tested during ohmic plasmas without additional heating. In addition, an external Li supply was also successfully tested, as were two novel flowing liquid Li limiter systems in HT-7. The first was a Li-metal infused trenches (LiMIT) system that exploited the thermoelectric magneto-hydrodynamic (TEMHD) effect to drive liquid Li flow [26], and second used a thin flowing film concept [27]. During this process, the practical techniques needed for handling liquid Li were also developed [28, 29]. It was observed that the influence of the liquid Li limiters on plasma performance was generally similar to that of Li coatings, i.e. increased plasma confinement, reduced impurity content, and reduced recycling. Compared with a free surface limiter, the Li limiter with a CPS-confined surface reduced Li droplet ejection into plasmas which otherwise could result in plasma disruptions. A re-filling experiment showed that liquid Li could be readily driven by pressured Ar, which is needed to increase the lifetime of the Li limiter.

Those successful experiments in HT-7 motivated the design of a more sophisticated Li limiter for use on EAST. The goal was to create a continuously flowing (with no interruptions) liquid lithium film in order to resolve the problem of contamination of Li surface monolayers by residual outgassing from the walls. Thus, a movable limiter with such a flowing liquid Li surface was designed for EAST. This limiter was also required to resolve technical questions that arose during the previous experiments, and it was designed to serve as a primary PFC in long-pulse H-mode plasmas with low recycling on EAST. This innovative approach addresses the programmatic goals of the EAST, and advances worldwide fusion energy and science development.

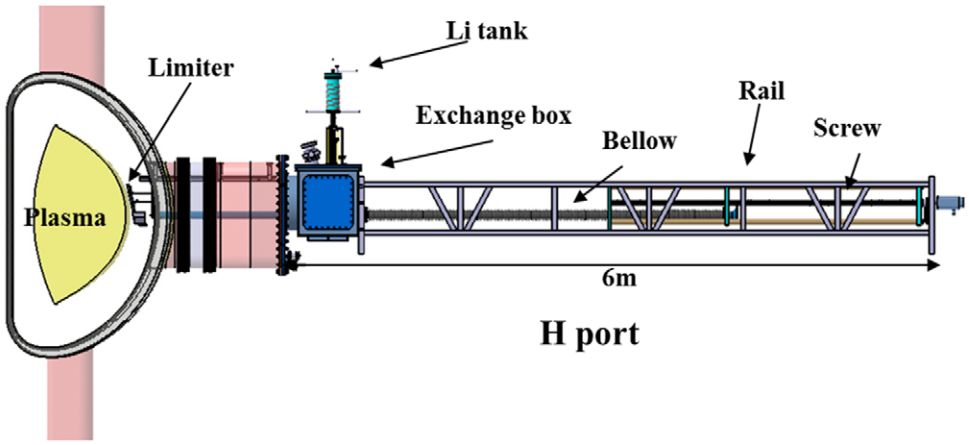

Figure 1. Overall structure diagram of the flowing Li limiter system on EAST.

In the remainder of this paper, we will present the main experimental results of the flowing Li limiter in EAST, including testing in L-mode and H-mode plasmas with auxiliary heating from lower hybrid wave (LHW) or neutral beam injection (NBI). The engineering design of the limiter and key components are described, and the experimental procedure is briefly introduced in section 2. Experiment results, including the flowing of Li on the stainless steel-coated copper plate, the interaction between the limiter and plasma, and the influence of the limiter on various plasma scenarios are presented in section 3. Conclusions are presented in section 4, touching on future upgrades for EAST, as well as the prospect of flowing liquid Li PFCs in future fusion devices.

2. Experimental set-up and procedures

2.1. Flowing liquid limiter system

The design of the FLiLi limiter for EAST is based on the concept of a thin flowing film that was previously tested in HT-7. The design implements both simplicity and safety for both structure and manufacturing. Exploiting the capabilities of the existing material and plasma evaluation system (MAPES) on EAST, the limiter was pre-wetted with Li and mechanically inserted to the boundary of EAST during plasma discharges. The limiter employs a novel electro-magnetic pump to drive liquid Li flow from a collector at the bottom of the limiter into a distributor at its top, and thus supply a continuously flowing liquid Li film to the wetted plasma-facing surface. For safety reasons, the design involves a minimum inventory of Li and uses only low hydrostatic (and electromagnetic) pressure to move that inventory. Further, no mechanical part or joint comes in contact with liquid Li to minimize effects of corrosion [30].

The flowing liquid limiter system was located at the *H* port on EAST, including a limiter head, a filling system, an exchange box, a collector, a limiter driving system, heating and cooling systems, and a power supply and control system, as shown in figure 1. The MAPES consists of a 5.8 m long steel scaffold and a step motor-activated drive screw, which can insert objects to the outboard edge of EAST plasmas [31].

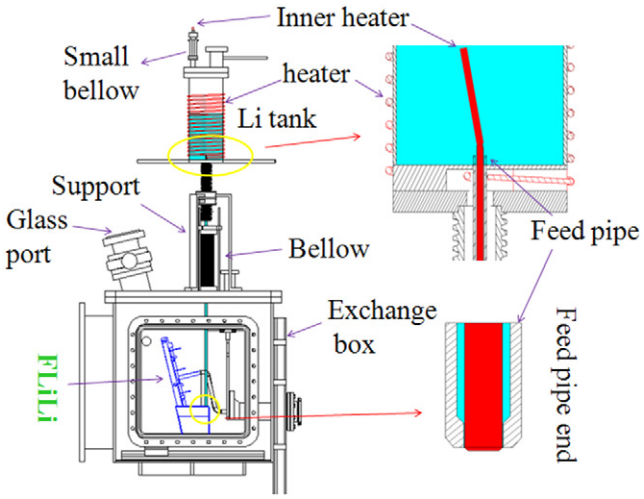

Figure 2. The Li filling system of the flowing liquid Li limiter on EAST.

In the case of the FLiLi limiter, the necessary copper electric lines, He cooling tubes and thermocouples are connected to the limiter assembly under high vacuum through the long welded bellows (2.6 m stroke). To prevent the vertical displacement of the conveyer rail caused by gravity, a quite robust support with guiding rails is installed on the top of the sector *H* to support the limiter with a pulley mechanism. The limiter can be moved in 2.5 m from the exchange box to the edge of plasma in the inner vessel of EAST. At the edge plasma, the limiter head could be moved to $r = 2.283$ m, i.e. 6.7 cm inside of the fixed Mo limiter in the machine.

A liquid Li supply system shown in figure 2, housed on the top of the exchange box, is designed to fill Li to the collector and to wet the front surface of limiter, prior to positioning the limiter into the EAST plasma vessel. A supply tank terminated by a vertical feed tube is movable via compression of the bellows. A window on an observation port allows for careful monitoring and positioning of the feed tube with respect to the insertion point on the collector. After filling solid Li into the supply tank, the feed tube is moved to the Li collector. With heating, the liquid Li will be filled to the collector, driven by Ar gas at suitable pressure. After the collector is filled with Li,

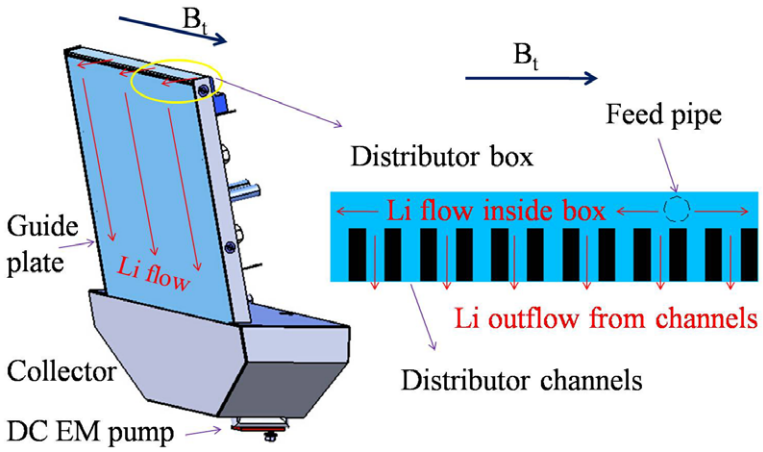

Figure 3. The sketch of the FLiLi limiter and Li distributor of FLiLi limiter on EAST.

liquid Li was pushed to the limiter plate for wetting of Li on SS plate by increasing of the Ar pressure. In the last step, the Li supply system is moved out for allowing the moving of the collector together with the limiter system to the plasma vessel of EAST.

As shown in figure 3, the limiter head is composed of a thick copper plate with heating and cooling channels serving as a thermal heat sink and stainless steel (SS) foil plate to support liquid Li. The copper plate has dimension, 350 mm long × 300 mm wide × 19 mm thick, and comprises the main body of the limiter. A thin (0.1 mm) SS foil brazed to the copper plate serves as a protective layer between liquid Li and the copper heat sink. In practice, liquid Li is expected to be guided by gravity and flow slowly ($<$10 mm s^{-1}) along the plasma-facing guide down to the collector. From this design, a thin film of liquid Li distributed uniformly on the whole of the SS plate is expected. For this purpose, the design contains a special distributor at the top of the limiter. The distributor is designed to provide a uniform supply of liquid Li into an array of 200 horizontal channels ($0.8 \times 0.8 \times 40$ mm^3) perpendicular to the toroidal magnetic field between the plasma-facing side and a distributor box filled with liquid Li on the back side of the copper plate. An inner EM pump at the bottom of the collector supplies a $J \times B$ force via a direct current between two electrodes, coupled to the toroidal magnetic field of the EAST device. Two 50 mm long electrodes are brazed to the upper and lower sides of the horizontal section of the near-vertical distribution tube. With a low voltage external voltage power supply, a dc current up to 100 A was projected, which is sufficient to drive Li upward on the plate at a rate of ~3 cm^3 s^{-1}.

The temperature of the limiter was controlled using three FeCrAl wires heaters and cooling channels embedded in the backside of the copper plate. In order to accomplish the initial wetting, a bulk plate temperature approaching 500 °C could be rapidly achieved, i.e. in 5–7 min. To ensure rapid cooling of the copper plate after wetting to limit Li evaporation, an active cooling system employing 5 MPa of circulating He gas in the cooling channels was implemented. Thus, temperature of the plate can be heated to higher than 500 °C for wetting of SS layer with Li, and also can reduced below 400 °C during plasma operation. The Li temperature is about 360–400 °C at the beginning of the plasma pulse. Thirteen thermocouples are attached at various locations on the plate's surface for the monitoring of the temperature distribution of the plate, which can be used for temperature feedback control, or for the calculation of the heat load from plasma. In this experiment, however, the cooling system was not used, i.e. the plate was inertially cooled.

The Li collector is a storage vessel of liquid Li which is separated from the bottom of the plasma-facing side of the copper plate by a small rectangular gap of 2 mm in the width, as shown in figures 3 and 7. This collector has a storage volume of 3.7 liters. A hole located on the top of the collector behind the copper plate is designed to engage with and to accommodate the feed tube at the bottom of the movable Li storage tank in the exchange box. An additional hole at the bottom of the collector leads directly into a near-vertical tube, which is used to supply liquid Li to the distributor at the top of the copper plate against gravity by the inner EM pump. The collector is open in the front of SS plate, which allows for re-collecting of liquid Li from the SS plate.

2.2. Diagnostic systems

Toroidal and poloidal distribution of the key diagnostics used in this experiment to evaluate plasma basic performance are shown in figure 4. Two CCD cameras are installed at the D port to respectively monitor looking to the limiter and opposite direction. The CCD looking to the limiter with a changing color due to the brightness is a black-white camera with about 120 Hz frame, and the other one looking to the opposite direction is a true color camera with 20 Hz frame. An integration of spectral diagnostics named 'filterscopes' with 50 kHz sampling rate viewing $D\alpha$, Li-I, Li-II, C-III, Mo-I, and visible Bremsstrahlung (VB) is installed at the G port to evaluate particle recycling and impurity content during plasma operation. The line-integrated radiated power is measured by 64 absolute extreme ultraviolet (AXUV) photodiode arrays located at P port to evaluate plasma total radiation level. An infrared camera located at K port is used to measure the surface temperature of the first wall surface directly. Divertor

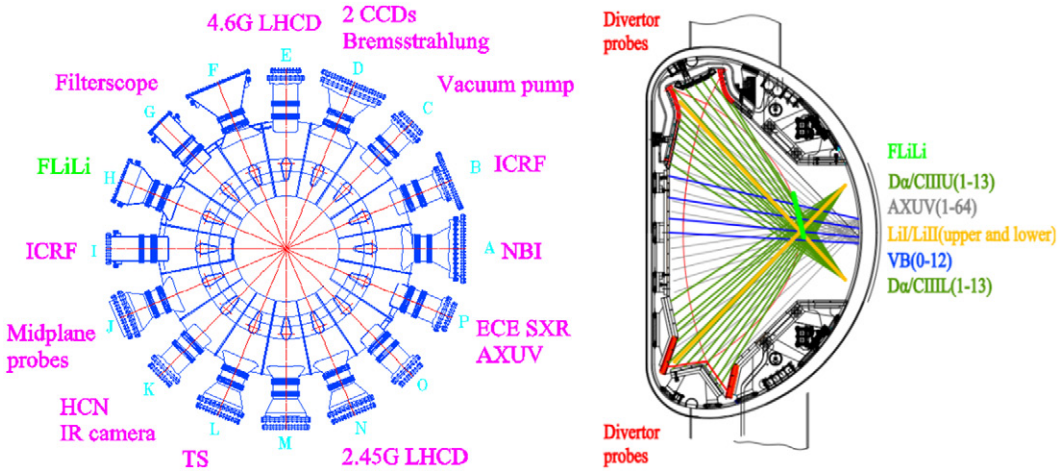

Figure 4. Toroidial (left) and poloidal (right) distribution of the key diagnostics and auxiliary plasma heating systems for the flowing Li experiment on EAST.

triple Langmuir probe (LP) arrays and a fast reciprocating LPs at the low-field side (LFS) mid-plane measured the particle and heat flux on the divertor targets, and the scrape-off layer (SOL) plasma characteristics.

2.3. Experimental procedures

Prior to the experiments, all critical mechanism, i.e. leak detection, MAPES driving mechanism, and baking, were tested without Li. After the FLiLi system was installed on EAST, the whole system was baked up to 500 °C for one day to release impurities. Then, the Li collector was filled with Li from an external overhead tank while housed in the exchange box. At this point, solid Li ingots with a total volume of 2.5 liter were deposited into the external tank. The feed tube was positioned and inserted into the hole on the top of collector. Solid Li was melted and the liquid Li flowed in the tube to the collector. After the collector was ~2/3 full, the feed tube was inserted into the hole in the bottom of the collector to fill liquid Li in the distributor box and all associated channels. Then, Ar with precisely controlled pressure was used to slowly push the liquid Li to flow onto the front plate of the limiter until the entire surface of the SS foil was wetted.

After the filling and wetting, the FLiLi limiter was moved to a vacuum chamber for continuous closed-loop operation using an electro-magnetic drive (i.e. $J \times B$) for Li circulation between the collector and the front surface of the limiter. During plasma experiment, various positions of the limiter, from $R = 2.374$ m to $R = 2.284$ m, were tested, shown in figure 5. Compared to the main fixed Mo limiter, the relative position corresponded from -24.2 mm to $+65.8$ mm, with the convention that positive values are nearer to the plasma. The limiter center was 12.27 cm above the mid-plane of EAST. The current passing the electrodes was varied from zero to 100 A, which equates to a pressure drive of up to 23.7 kPa. This provides up to ~4.3 $\mathrm{cm}^3\ \mathrm{s}^{-1}$ of Li upstream flow from the collector to the distributer, given the toroidal magnetic field of 1.9 T.

The parameters for these discharges are as follows: plasma current $I_\mathrm{p} = 0.4$ MA, toroidal magnetic field $B_\mathrm{T} = 1.9$ T, central

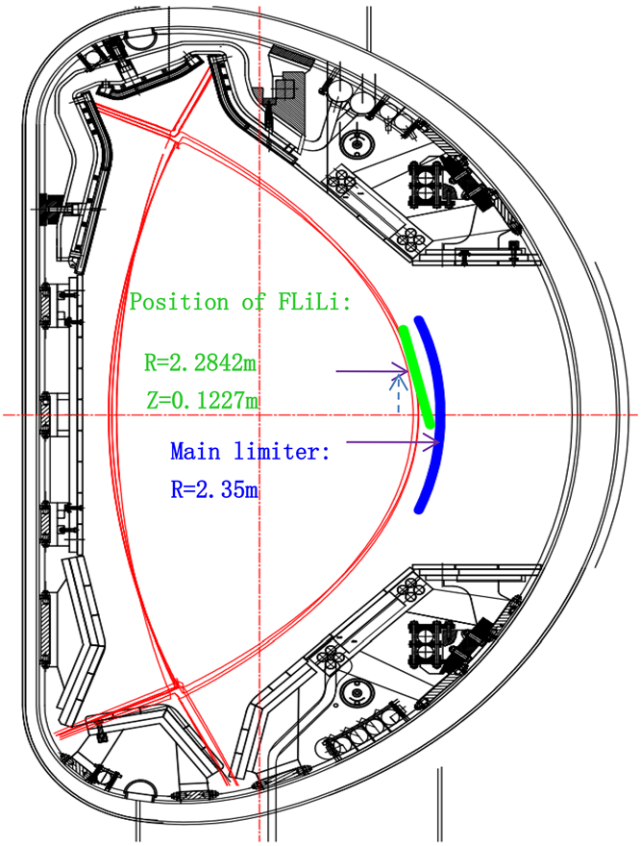

Figure 5. The position of the flowing liquid Li limiter in EAST.

density n_e was varied between 1.3 and 6.2×10^{19} cm^{-3}, and central electron temperature $T_\mathrm{e}(0) = 1.1$ keV. Plasmas were in the lower single-null configuration, with elongation $\kappa = 1.6$ and lower triangularity $\delta = 0.54$. Auxiliary heating power was provided by LHW heating from 0.3 to 0.65 MW, and NBI heating from 1.15 to 1.3 MW, either separately or together. We note that just before the FLiLi experiment, the wall had been coated by a cumulative total of 2.9 kg Li via evaporation from three uniformly placed ovens; the evaporation was routinely carried out each morning for 82 d.

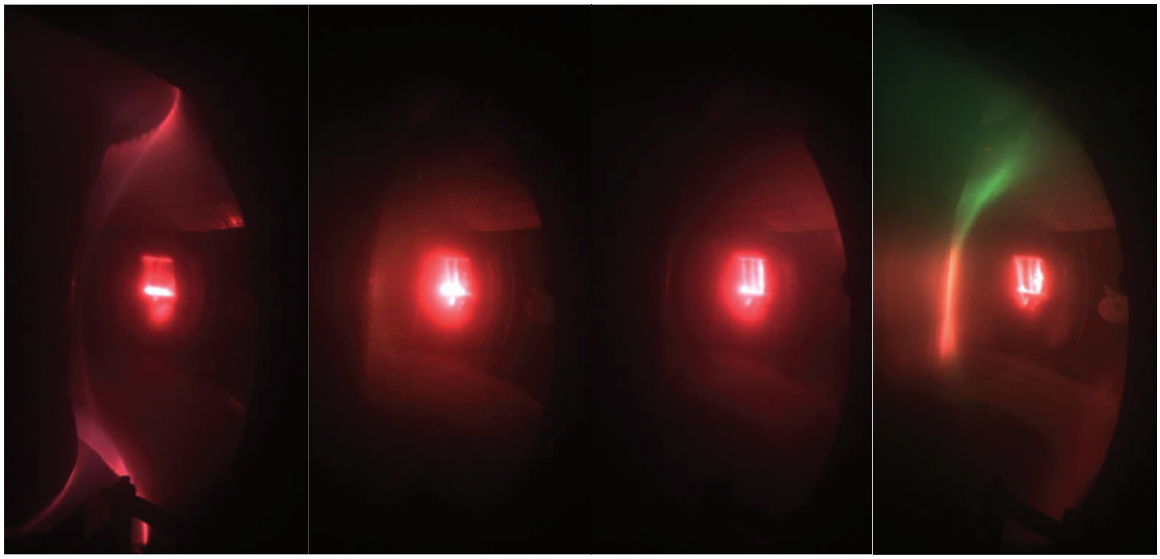

Figure 6. Flowing of Li on the surface of SS foil plate at the initiation of plasmas at 0.2 s with various EM driving current in the inner EM pump ($B_T = 1.9$ T; Li limiter at $R = 2.284$ m). (*a*) Without current, (*b*) 20 A, (*c*) 40 A, (*d*) 80 A.

3. Main results

3.1. Flowing of Li on the stainless steel foil plate

In principle, if the EM drives pressure is larger than the gravity pressure drop, liquid Li can flow upward from the feed pipe to the distributor. The magneto-hydrodynamics (MHD) drop in the supply pipe behind the copper heat sink can be assessed as [30]:

$$\Delta P^{\mathrm{FP}} \cong 16\,000\, V_{\mathrm{cm\,s^{-1}}}(d/a)B_{\mathrm{t}}^2 L_{\mathrm{m}}. \quad (1)$$

where $V_{\mathrm{cm\,s^{-1}}}$, d, a, B_{t} and L_{m} are the flow rate of liquid Li, wall thickness of the feeding pipe, inner radius of the supply pipe, EAST toroidal magnetic field, and equivalent length of the feed pipe respectively. Based on design parameters of the EAST FLiLi limiter, this pressure can be simplified to $\Delta P^{\mathrm{FP}} \cong 800 V_{\mathrm{cm\,s^{-1}}} B_{\mathrm{t}}^2$. The gravitational pressure drop along the feed pipe is about 1500 Pa calculated by the formula: $\Delta P^{\mathrm{gravity}} = \rho g h$.The electric current driven externally normal to the vertical flow creates a pressure [30]:

$$\Delta P^{j\times B} = 100(I_{\mathrm{A}}/\omega_{\mathrm{cm}})B_{\mathrm{t}} \quad (2)$$

Where I_{A} is the current across the flow, and ω is the horizontal width of the flow.

In the present experiment, the current passing through the cathodes was increased sequentially from zero to 100 A, in intervals of 20 A, which can produce about 4760 Pa of driven pressure, i.e. higher than the gravitational pressure drop (~1500 Pa). This corresponds to ~0.46 $\mathrm{cm^3\ s^{-1}}$ of the Li upstream flow from the collector to the distributor. Figure 6 shows the emission of Li light from the surface of the SS foil plate with various driving current values during discharges. Li flow on the plate, e.g. as indicated by the vertical filamentary stripes, was evident even at the lowest current of 20 A. Three hours of uninterrupted Li flow including seventeen tests

Figure 7. The picture of the FLiLi limiter surface taken in the air after the campaign of EAST.

with plasmas was demonstrated in this manner. It confirms the validity of the calculating method and its potential usefulness for conceptual designs of future massive liquid Li application in fusion devices.

In the absence of driving current, there is a bright horizontal line along the center of the limiter, responding to the location of the interaction of plasma and this limiter (figure 6(*a*)). When driving current was added, the bright lines were vertically oriented, indicating the interaction of plasma changed along the Li flow direction. With the increase of the driving current, the Li flow rate increased, which eventually flowed down the front face of the limiter into the collector. Thus the EM pump and gravity formed a closed, recirculating Li flow loop. Moreover, it was found the flow rate of the liquid Li was controlled by adjusting the current. We note that while droplet ejection was nearly eliminated, a few droplets with diameter of ~3–5 mm were ejected from the collector during the

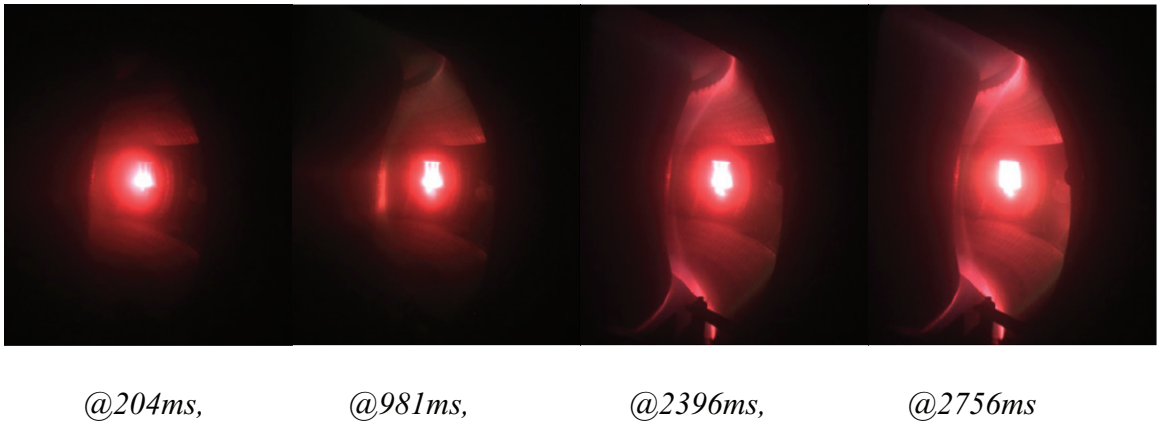

Figure 8. Evolutions of color near the FLiLi limiter surface during plasma start-up phase in shot #52692.

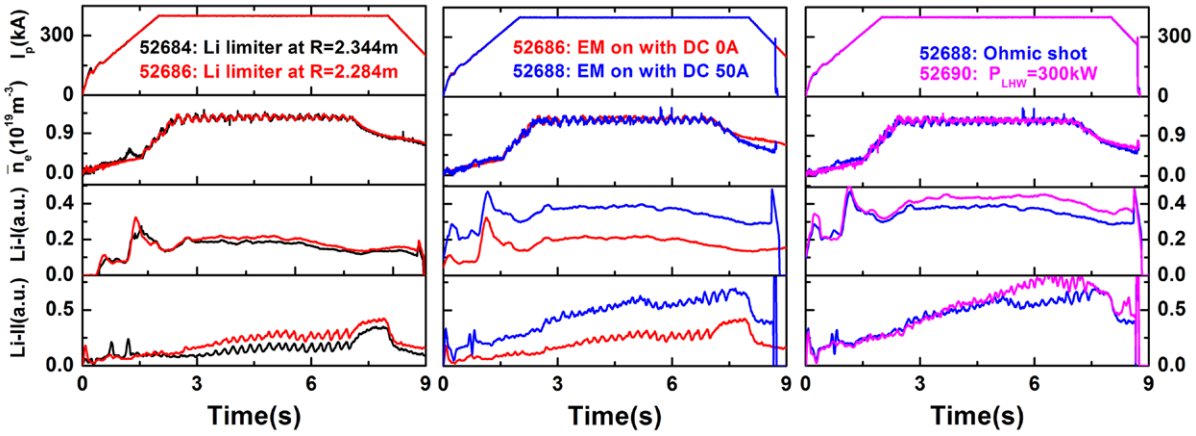

Figure 9. Li emission versus on various of the radial positions of the limiter (left), EM driven current (mid) and the heating power of plasma (right, The additional heating was started at 2.7 s and ended at 8.5 s).

discharge sequence. In summary, the design of the EM pump was successful for closed-loop, flowing liquid Li system in EAST.

As seen in figures 6(*b*)–(*d*), the bright vertical lines on the plate indicate a strong interaction of flowing Li with plasma at the initiation of plasmas with weak interactions. The vertical lines in the images are likely individual Li streams. After the experiment, we checked the surface of the plate and found about ten vertical streak patterns with widths from 10 mm to 40 mm (figure 7). The fractional coverage of the streams is only about 30% of the width of the plate, indicating the flow was not uniform. One possible reason for this non-uniformity is that the feed channels in the distributor are themselves not quite uniform. This could cause the channel-to-channel flow resistance to differ. Li would naturally flow along those channels with the lowest resistance. After the initial formation of streams, the Li might have wet on those channels and further reduced the flow resistance, due to surface tension. This might have made it more difficult for the Li streams to wet the entire front surface, resulting in the observed streak patterns.

3.2. Interaction of flowing Li with plasma

As mentioned in section 3.1, the bright lines on the limiter indicated the interaction locations between plasma and the flowing Li, and these lines were different at the various applied dc currents. After the start-up of the plasma, the plasma-wall interactions at the limiter became stronger until the surface of the limiter was observed. Figure 8 gives an example of the interaction evolving in shot #52692. As the discharge evolved, the small zone of bright white light, with apparent discrete vertical flow channels, expanded to fill the entire surface of the limiter at 2.756 s. At this time, the intensity of the Li-II emission also increased.

Optical spectrometers enabled measurement of both Li-I and Li-II emission. The Li-I line emitted by neutral Li atoms at 670.8 nm is in the red portion of the visible spectrum. The Li-II line emitted by Li^+ ions at 548.4 nm emits a green color. When Li was flowing on the limiter, both Li-I and Li-II emission became strong, i.e. when Li was released from the limiter due to strong plasma-wall interaction. It was found that intensity of the Li emission depended on the radial position of the limiter, the current driven by the EM Li pump, and also on the auxiliary heating power delivered to the plasma.

Figure 9 (left panels) compares the emission from the limiter at radii of 2.344 m and also ~6 cm closer to the plasma; the emission from $R = 2.284$ m is 10–50% higher. A 50 A current driven by the EM pump also increased the Li emission by ~100% (figure 9—middle panels); the Li flow rate is controlled by this driving current. Finally with an increase of the

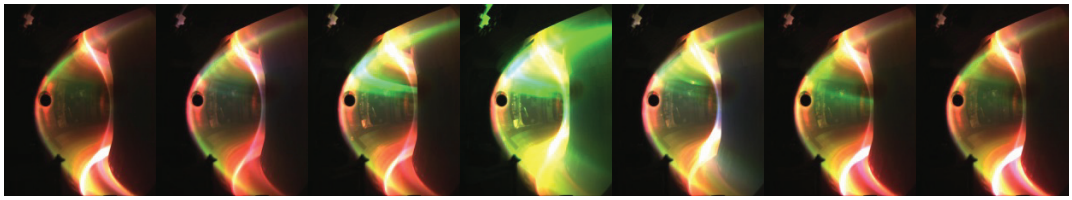

@4.135, @4.233, @4.282, @4.332, @4.381, @4.431, @4.479

(a)

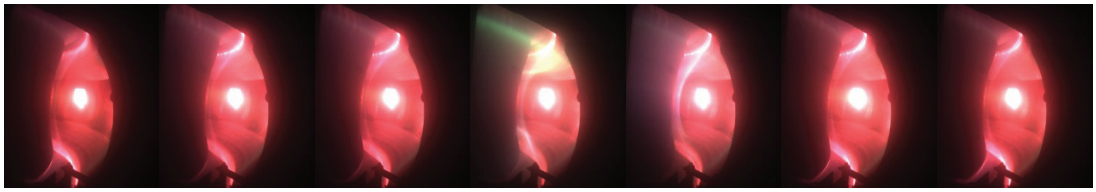

@4.135, @4.233, @4.282, @4.332, @4.381, @4.431, @4.479

(b)

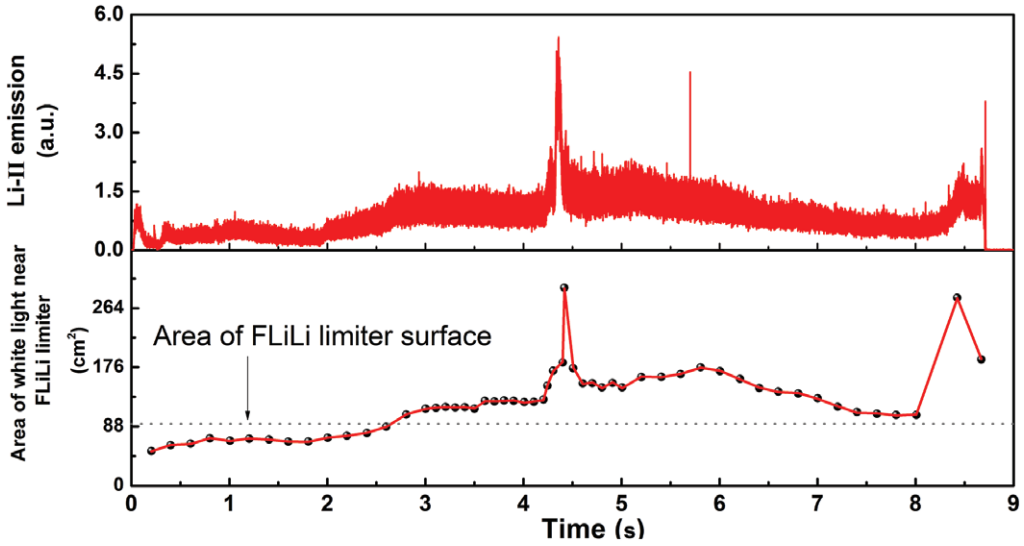

(c)

Figure 10. A burst of Li emission during strong interaction between plasma and the limiter. The FLiLi limiter is at $R = 2.284$ m; the driving current of the inner EM pump is 20 A; $I_p = 0.4$MA; $n_e = 2.6 \times 10^{19}$ m^{-3}; lower hybrid heating power = 600 kW. (*A*) CCD picture looking to the opposite direction ofthe limiter(From port D to A), (*B*) CCD picture looking directly to the limiter (from port D to H), (*C*) Evolutions of area of bright white color near the limiter and Li-II emission.

auxiliary heating power, the emission of Li became marginally stronger (figure 9—right hand panels). This last dependence seems reasonable, due to higher heat flux of plasma impinging on FLiLi, which served as the main limiter in these comparsion discharges.

Occasionally, a burst of white light, representing a strong interaction between plasma and the limiter, would spontaneously occur. In this case, the entire surface of the FLiLi limiter glowed bright, e.g. figure 10 in shot #52692. Note that both the area and the intensity increased during this burst. We speculate that, when a continuous heat flux comes from plasma, the temperature of the liquid Li would increase. At sufficiently high temperature, bubbles would have formed possibly due to strong evaporation, and the bursting of these bubbles would reduce the surface temperature. This seems that the temperature of FLiLi limiter should have been clamped by the formation of bubbles. In addition to Li transport to the divertors, a clear green layer with strong Li^+ emission at the same poloidal position as the limiter was observed toroidally opposite direction of the limiter location. Simultaneously, the influx of Li to the plasma increased by a factor of 3, as found by integrating optical spectroscopy measurements. These measurements

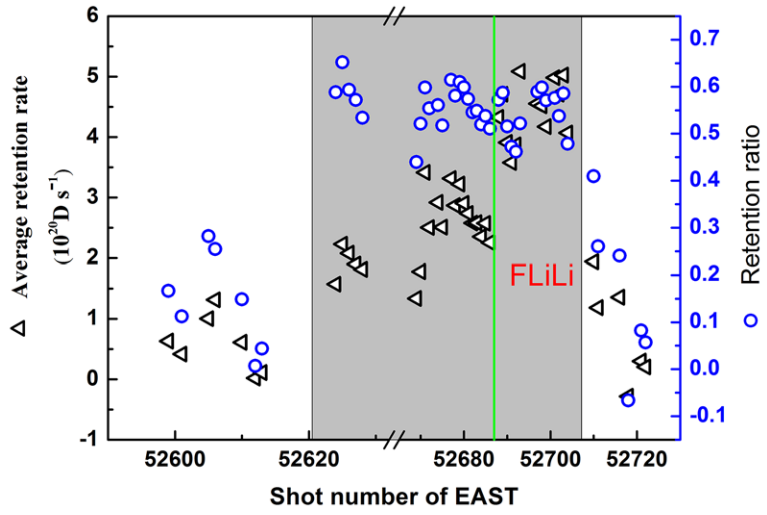

Figure 11. Evolution of wall retention rate and ratio as function of shot number during the FLiLi limiter experiment (black symbol is average retention rate and the blue symbol is retention ratio).

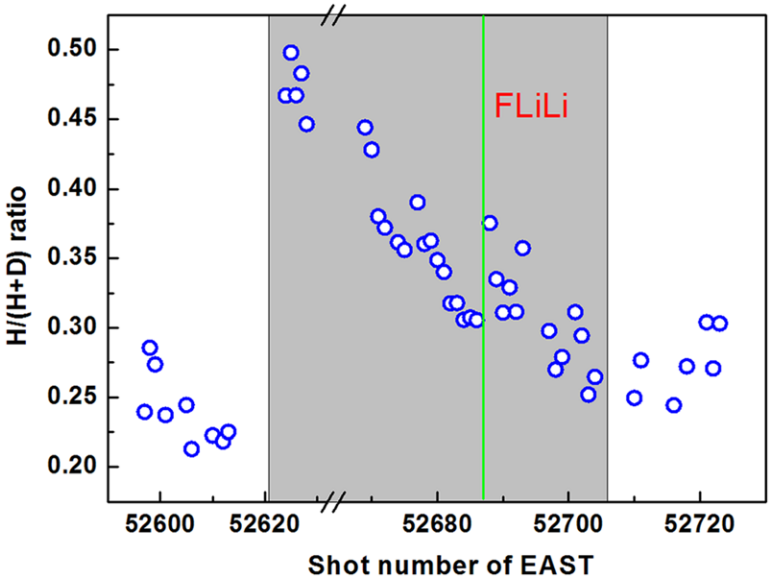

Figure 12. Evolution of the $H/(H+D)$ ratio as function of shot number during the FLiLi limiter experiment.

suggest that when Li was released from the limiter surface, most of the Li was transported along the toroidal direction of EAST. It is believed that the layers with strong Li/Li^+ emission from FLiLi would reduce the interaction between plasma and PFCs that form the substrate under liquid Li.

Clear damage was observed on the FLiLi plate after retraction from EAST, e.g. as shown in figure 7. This damage was primarily on the on the ion drift side, i.e. in the direction of the neutral beam injection, with obvious modification of the stainless steel foil coating on the copper heat sink. In parts, the SS foil was completely eroded, allowing Li to attack the copper substrate. The heat flux to FLiLi under these conditions, i.e. auxiliary heating of 1.95 MW, should have resulted in a peak, relatively modest value ~0.8 MW m^{-2}. Thermal calculations project a temperature of 474 °C in 10 s with a fully functional cooling system, or 771 °C with a damaged cooling system, assuming an initial temperature of 400 °C. We therefore speculate that bombardment of the plate by high energy ions caused the damage. However, the primary candidate to explanation is a possibly uneven brazing of 0.1 mm foil and copper, which left voids and, thus, exposed the foil with no heat sink contact to the plasma heat flux and caused the observed limiter surface modifications.

3.3. Reduction of recycling and impurities, and increase of fuel retention

As expected from the results of the FLiLi experiments on HT-7, recycling was reduced while the ratio of hydrogen in the plasma, defined as $H/(H+D)$, was reduced with increasing shot number, while fuel retention increased during FLiLi operation.The high capacity of Li to retain hydrogen isotope is well known. It should be noted here that the retention ratio (defined as the fraction of fuel retained on the walls divided by the total fuel) increased in the first plasma with the liquid Li limiter after wetting, and remained high at ~60% with FLiLi

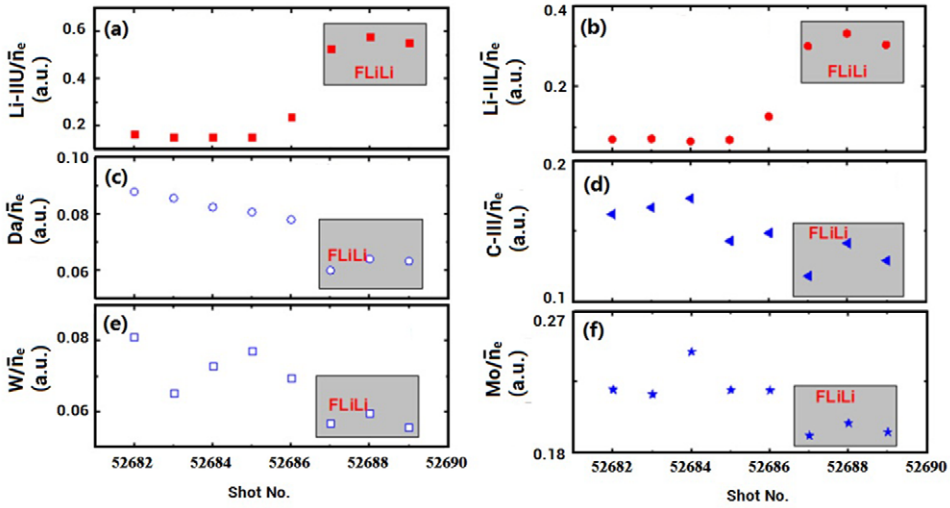

Figure 13. Evolutions of recycling and impurities in ohmic discharges during the FLiLi limiter experiment (Ohmic heating only, $I_P = 0.4$ MA; $n_e = 1.2 \times 10^{19}$ m^{-3}, same plasma configuration as in figures 11 and 12). Shown are the (*a*) Li-II line emission intensity from the upper divetor, (*b*) Li-II line emission intensity from the lower divetor, (*c*) Dα line emission intensity, (*d*) C-III line emission intensity, (*e*) W line emission intensity and (*f*) Mo line emission intensity, with all these signals normalized to line-averaged electron density.

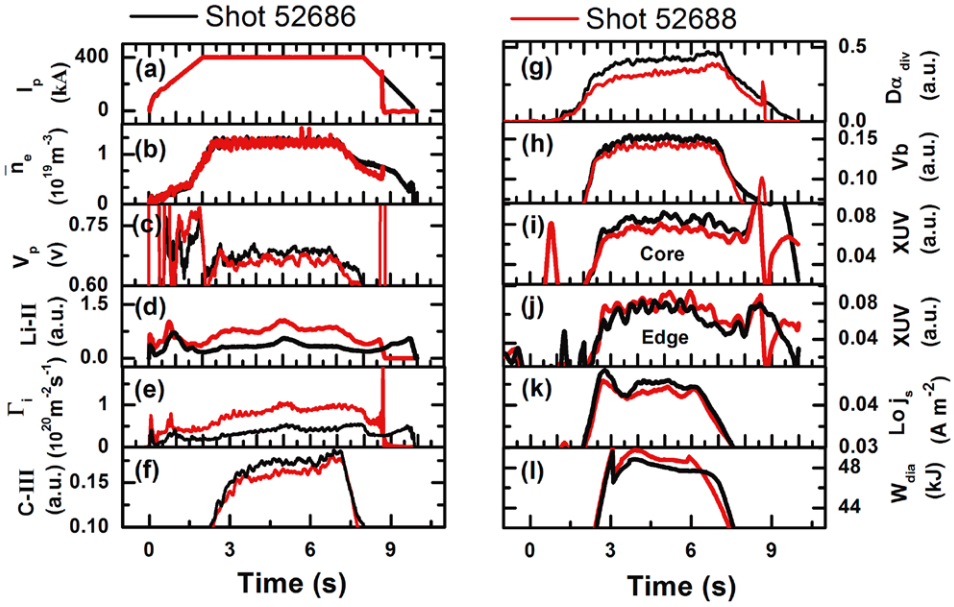

Figure 14. Comparsion of two ohmic plasma during the FLiLi limiter experiment with or without active Li flowing (Ohmic heating only, $I_P = 0.4$MA; $n_e = 1.2 \times 10^{19}$ m^{-3}, LSN). Shown are the (*a*) plasma current, (*b*) line-averaged electron density, (*c*) loop voltage, (*d*) Li-II line emission intensity, (*e*) influx of Li into plasma calculated from Li line emission, (*f*) C-III line emission intensity, (*g*) $D\alpha$ lineemission intensity from the divetor, (*h*) visible bremsstrahlung, (*i*) XUV radiation in core, (*j*) XUV radiation in edge, (*k*) ion saturation current density at lower outer divertor target and (*l*) plasma stored energy.

operation. The retention rate, which depends on specific discharge plasma parameters like density and pulse length, also showed a moderate increase. When we started to drive Li on the surface of the limiter applying the inner EM pump with the driving current from shot #52687(vertical green line in figure 11), the average retention rate increased again from 2.25×10^{20} s^{-1} to 4.33×10^{20} s^{-1}, while the retention ratio was unchanged. After deactivating FLiLi, both the retention rate and ratio decreased over ~5 discharges, which indicates that the fresh Li on the limiter or deposited onto other PFCs was reduced step-by-step.

At the same time, the ratio of $H/(H + D)$ was gradually reduced from 50% to 25% (figure 12), similar to the effect of Li coatings in EAST [32].The jump in hydrogen fraction just before the FLiLi experiment was caused by a two-day long period without discharges, which normally causes an increase of the $H/(H + D)$. Also the high operating temperature of FLiLi caused the outgassing of the limiter and nearby first wall regions, which also caused an increase of the $H/(H + D)$ ratio. During the discharge sequence using the FLiLi limiter, $H/(H + D)$ ratio gradually but continuously reduced. After shutdown of the FLiLi limiter, $H/(H + D)$ ratio rose again.

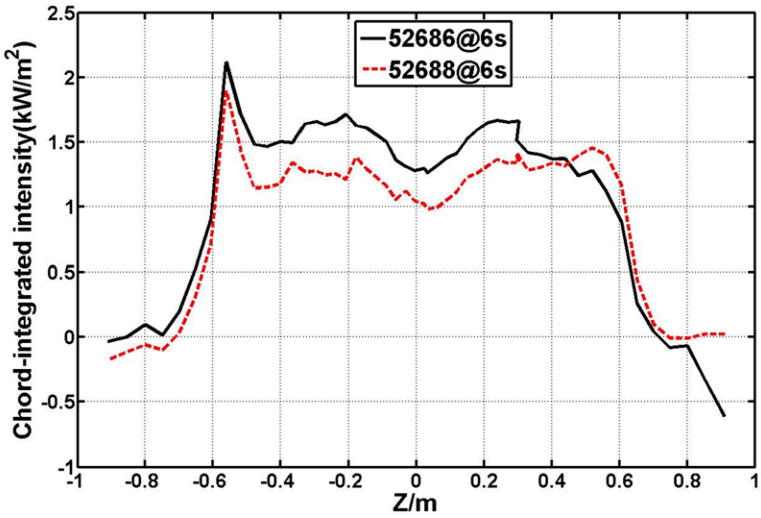

Figure 15. Comparision of radiated power profiles during plasma discharges at 6 s with or without active Li flowing.

At the beginning of the application of 20 A driving current, the Li-II emission increased by a factor of 6, as shown in figure 13. At the same time, particle recycling was clearly reduced by about 33%. In addition impurities including C, Mo, and W, most coming from plasma facing materials of the first walls and divertor, were reduced during the FLiLi operation. This indicates the FLiLi is beneficial for the control of recycling and impurities in plasma, which is also similar to the effect observed from fresh evaporative Li coatings in EAST.

3.4. Effect of the FLiLi limiter on plasma discharges

Figure 14 compares two ohmic plasmas with (shot #52688, red traces) and without (shot #52686, black traces) active Li flowing of the FLiLi limiter. It is clear that with actively flowing liquid Li, loop voltage (V_p) slightly decreased and stored energy (W_{dia}) slightly increased. In addition, actively flowing Li flowing led to a modest ~16% reduction in the divertor $D\alpha$, representing a measureable reduction in target plate recycling. The influx of Li to plasma, calculated from Li-II emission, was 2.5 higher with FLiLi, and also increased during the discharge, probably due to the heating of the liquid Li from plasma-wall interactions.

As seen in figure 15, with actively flowing Li, the radiation in the core plasma is modestly lower than that in the discharge without active flowing Li. It can also be seen (figure 16) that with flowing Li, the edge electron temperature decreased, and peaked slightly in the center. The possible reason for the decrease of edge T_e is too high Li radiation from the FLiLi limiter, which is different from that in the case of Li coating with low edge recycling; the reason for the core peaking of T_e is not yet understood.

As discussed in section 3.2 and shown in figure 10, a strong emission burst from the FLiLi limiter sometimes occurred during discharges. Those individual bursts also transiently influenced the plasma performance. As shown in figure 17, the plasma density increased from 1.6×10^{19} m^{-3} to 2.5×10^{19} m^{-3} during the Li burst. This indicated the emitted Li fueled the plasma and probably almost 100% of the additional

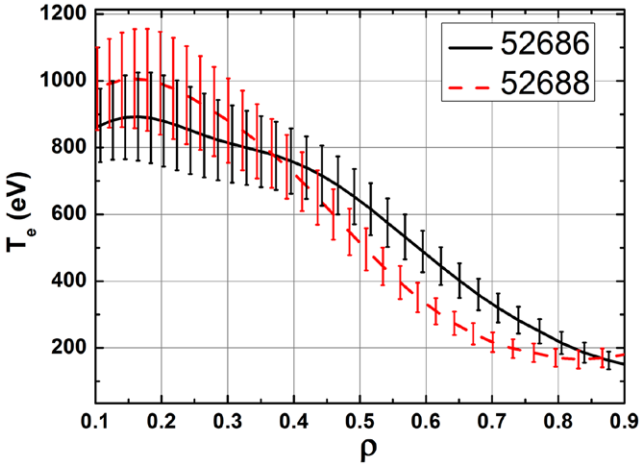

Figure 16. Comparision of T_e profiles during plasma discharges at 6 s with or without active Li flowing.

density originated from the Li. The intensity of C-III emission and $D\alpha$ from the divertor was simultaneously reduced, suggesting that carbon impurities and particle recycling were mitigated. Somewhat surprisingly, both the radiated power and stored energy increased as well, suggesting that the Li burst from FLiLi was somehow beneficial for the improvement of core confinement.

During the Li burst from the FLiLi limiter, Langmuir probe measurements showed that the edge electron temperature (T_e) near last closed field surface (LCFS) decreased while the n_e increased, as shown in figure 18. This is likely due to a large amount of Li entering plasma. During the emission burst, the increase of n_e exceeds the reduction of the T_e, leading to higher plasma pressure (figure 18(c)). Infrared thermography showed an decreased surface temperature at the inner divertor plate during the burst as shown in figure 19. The reduction of the temperature at the inner divertor plate during the burst suggests that the enhanced Li radiation reduced the divertor heat flux. Indeed, it was also found that the heat load, indicated by ion saturation current measurements from the diverter Langmuir probes, was significantly reduced during the Li burst.

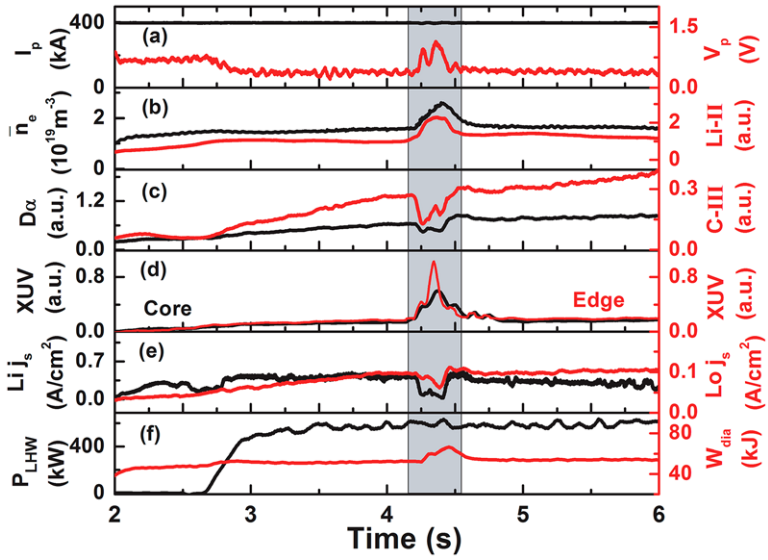

Figure 17. Plasma parameters evolution of a plasma (#52692) with Li burst during FLiLi limiter experiment. Shown are the (*a*) plasma current and loop voltage, (*b*) line–averaged electron density and Li-II line emission intensity, (*c*) $D\alpha$ and C-III line emission intensity, (*d*) XUV radiation in core and in edge, (*e*) ion saturation current density at lower inner and outer divetor targets and (*f*) LHW heating power and plasma stored energy.

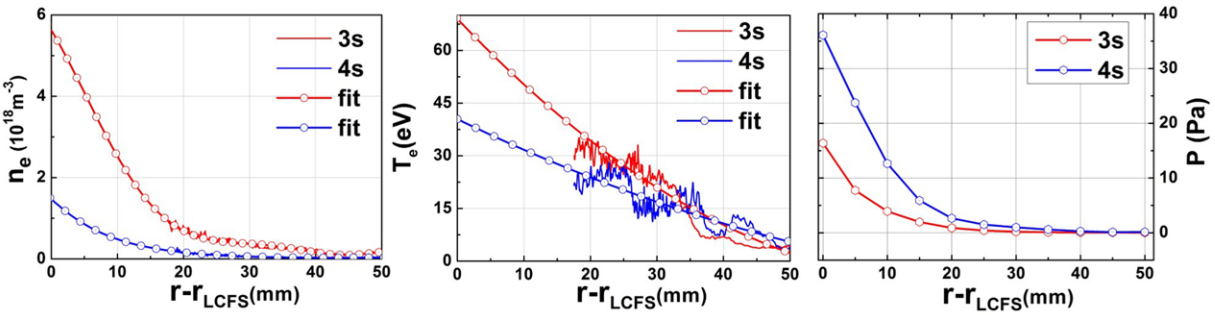

Figure 18. Edge plasma parameters before and during the Li burst during FLiLi limiter experiment. (*a*) density profile, (*b*) temperature profile and (*c*) plasma pressure profile.

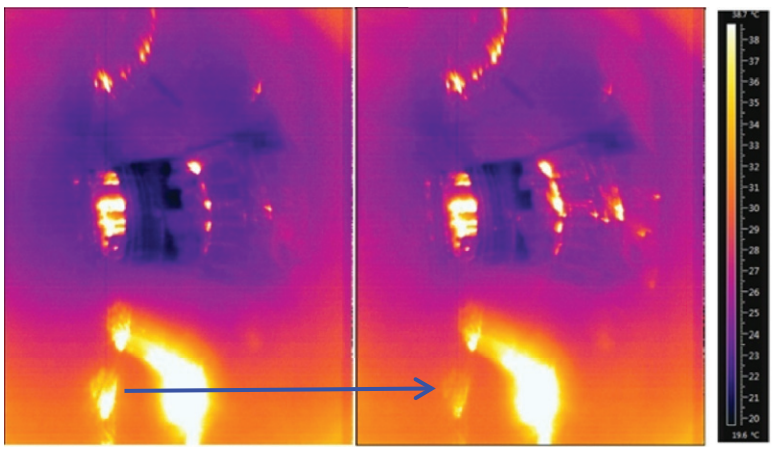

Figure 19. Surface temperature at the divertor in plasma (#52692) during FLiLi limiter experiment, (*a*) before the Li burst, (*b*) during the Li burst).

It was found the FLiLi limiter is compatible with various auxiliary heating schemes. H-mode plasmas were obtained by NBI and LHW heating while using the FLiLi limiter. As shown in figure 20, two types of H-mode plasma discharges ($B_T = 2$ T, $I_p = 400$ kA, $n_e = 3 - 3.5 \times 10^{19}$ m^{-3}, $P_{LHCD} = 600$ kW, $P_{NBI} \sim 1.3$ MW, LSN configuration,

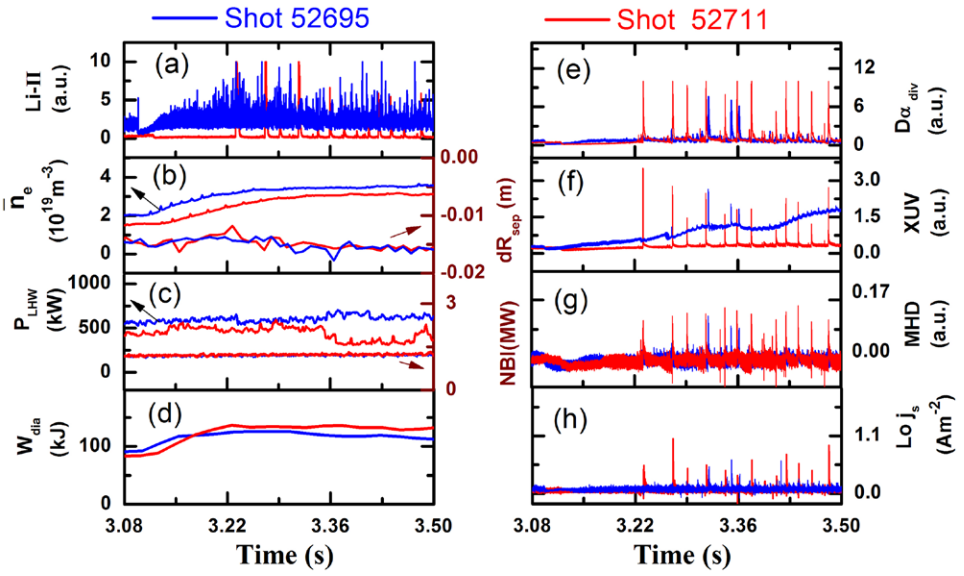

Figure 20. Comparison of two H-mode plasmas with (shot #52695) or without (shot #52711) active Li flowing. Shown are the (*a*) Li-II line emission intensity, (*b*) line–averaged electron density and the radial separation of X-points mapped to the outer mid-plane, (*c*) LHW and NBI heating power, (*d*) plasma stored energy, (*e*) $D\alpha$ line emission intensity, (*f*) XUV radiation in plasma core, (*g*) MHD signal from the Mirnov magnetic pickup coil signal and (*h*) ion saturation current density at the lower outer divertor target.

elongation $k = 1.59$, triangularity $\delta = 0.47$) are compared. It was found that baseline of Li emission strength in shot 52695 with the FLiLi limiter was ~6 × higher than that in shot 52711 without the FLiLi limiter. The baseline of the XUV signal, which correlated with radiated power, is also high in the plasma with the FLiLi limiter. There were many spikes of Li emission during H-mode plasmas in both cases. When using the FLiLi limiter, the spikes did not correlate with ELMs, whereas all of the Li emission spikes were correlated with ELMs without the FLiLi limiter. This suggests that Li light mostly came from the FLiLi limiter when it was inserted as the main limiter, whereas it mostly came from the Li pre-coated wall when the FliLi limiter was retracted. There were fewer ELMs with smaller $D\alpha$ amplitudes with the FLiLi limiter than without, as shown by divertor $D\alpha$ emission. It should be noted that the $D\alpha$ emission spikes in the plasma without the FLiLi limiter were saturated. Additionally, ELM-free phase of several tens of ms and up to 150 ms were observed with the FLiLi limiter. At the same time, MHD activity was suppressed and the ion saturation current on the divertor Langmuir probes was reduced with the FLiLi limiter. Clearly use of the FLiLi limiter as the main plasma limiter inside of the nominal separatrix is compatible with H-mode plasmas, and also seems to mitigate ELMs. This result is qualitatively similar to the results of Li aerosol injection to produce long pulse H-mode plasmas devoid of large ELMs in EAST [15]. Even though the FLiLi limiter could not fully suppress ELMs, short ELM-free phases were observed, with comparable Li emission between FLiLi limiter operation and that observed during Li aerosol injection. We speculate that the FLiLi limiter has an active coating effect on plasma facing surfaces, similar to that during Li aerosol injection.

4. Discussion and summary

A continuously flowing liquid Li limiter based on the concept of a thin flowing film, has been successfully designed and tested in the EAST device. The experiment was performed at the end of a run campaign, with substantial accumulated in-vessel Li inventory from preceding daily evaporations. The present experiment confirms that the liquid Li can be driven by built-in dc EM pumps to form a recirculating, closed loop system for fusion devices. Further, it is also found the flow rate of liquid Li could be controlled by adjusting the dc current. By using the FLiLi limiter, a modest improvement of plasma performance was obtained, as indicated by reduced core impurity radiation and hydrogen recycling. A strong yet controllable Li emission layer at the plasma edge was observed with the FLiLi limiter, due to the strong interaction between the liquid Li surface and plasma. This interaction effectively reduced particle and heat flux onto the divertor plate, and was accompanied by a slight increase of stored energy. Even though the FLiLi limiter was itself damaged in contact with the plasma, the limiter was shown to be compatible with plasmas with various auxiliary heating schemes. Specifically H-mode plasmas via NBI and LHW heating were maintained while using the FLiLi limiter. Also, ELMs could be partially mitigated using the FLiLi limiter, with evidence of short (<150 ms) ELM-free phases.

Most discharges ran normally without visible Li droplet ejections, and very few disruptions were observed. Even in the discharges terminated by disruptions, it was difficult to observe Li droplets. Following this experiment on the last day of the run campaign, only a few droplets with small size were found on the vacuum vessel surface around the FLiLi limiter. This differs from the results of liquid Li limiter with free surface [33], but is similar to experiments using the CPS structure

or FLiLi limiter with thin Li film [34]. Evidently the strong surface tension due to the thin Li layer withstood the EAST electromagnetic forces, and thus prevented Li ejection.

During the FLiLi limiter experiment in EAST, occasional Li emission bursts were observed from the limiter, reflecting a strong interaction between liquid Li and the plasma. In this case, the light intensity from the limiter increased, and a strong green emission belt appeared, and diffused toroidally away from the FLiLi limiter. This layer seemed to insulate the plasma from the wall, decreasing the surface damage and reducing impurity release from the wall materials. Additionally, the impurity and fueling particles that were released from the wall might have been screened by this Li layer. These results are similar to those from T-11M and FTU with liquid Li systems [35, 36] and active Li powder injection on EAST [15] and DIII-D [16]. On T-11M and FTU, a toroidally-extended Li radiation loop was also observed. In those devices, ~80% of input power was radiated from the edge plasma to effectively protect the Li limiter during 2000 pulses.

Several issues encountered in this experiment require resolution. First, uniform wetting of the SS foil plate needs to be demonstrated. This should lead to uniform Li flow on the limiter. Second, the damage of the SS foil plate needs to be understood and eliminated. Good thermal contact between the SS plate and the copper heat sink needs verification via thermography. Alternately a heat sink made of a refractory metal compatible with Li may be preferable. Finally, a reliable temperature control system with heating and cooling is required. Cu or Fe lines, possibly come from the limiter plate, should be real-time measured during FLiLi experiment to inform the damage of the limiter and to avoid the risk of leaks. These upgrades should enable the FLiLi limiter to operate in long pulse plasmas with high heating power.

Acknowledgments

This research was funded by National Magnetic confinement Fusion Science Program of China under Contract No.2013GB114004, National Nature Science Foundation of China under Contract No. 11321092 and No. 11405210, and the JSPS-NRF-NSFC A3 Foresight Program in the field of Plasma Physics (NSFC No.11261140328). The PPPL and LiWallFusion co-authors were supported by U.S. Dept. of Energy contract DE-AC02-09CH11466.

References

[1] Tsitrone E. 2007 *J. Nucl. Mater.* **363–5** 12
[2] Loarte A. *et al* 2007 *Nucl. Fusion* **47** S203
[3] Li J. *et al* 2013 *Nat. Phys.* **9** 817
[4] Zohm H. *et al* 2013 *Nucl. Fusion* **53** 073019
[5] Zakharov L.E. *et al* 2007 *J. Nucl. Mater.* **363–5** 453
[6] Coenen J.W. *et al* 2014 *Phys. Scr.* **T159** 7
[7] Mansfield D.K. *et al* 1996 *Phys. Plasmas* **3** 1892
[8] Sanchez J. *et al* 2011 *Nucl. Fusion* **51** 10
[9] Battaglia D.J. *et al* 2013 *Nucl. Fusion* **53** 113032
[10] Maingi R. *et al* 2009 *Phys. Rev. Lett.* **103** 075001
[11] Kugel H.W. *et al* 2008 *Phys. Plasmas* **15** 056118
[12] Bell M.G. *et al* 2009 *Plasma Phys. Control. Fusion* **51** 124054
[13] Canik J.M. *et al* 2011 *Phys. Plasmas* **18** 056118
[14] Maingi R. *et al* 2012 *Nucl. Fusion* **52** 083001
[15] Hu J.S. *et al* 2015 *Phys. Rev. Lett.* **114** 055001
[16] Osborne T.H. *et al* 2015 *Nucl. Fusion* **55** 063018
[17] Majeski R. 2005 *Nucl. Fusion* **45** 519
[18] Tuccillo A.A. *et al* 2011 *Nucl. Fusion* **51** 094015
[19] Jaworski M.A. *et al* 2013 *Nucl. Fusion* **53** 083032
[20] Mirnov S.V. *et al* 2006 *Plasma Phys. Control. Fusion* **48** 821
[21] Schmitt J.C. *et al* 2015 *Phys. Plasmas* **22** 056112
[22] Wan B. *et al* 2013 *Nucl. Fusion* **53** 104006
[23] Guo H.Y. *et al* 2014 *Phys. Plasmas* **21** 056107
[24] Zuo G.Z. *et al* 2012 *Plasma Phys.Control. Fusion* **54** 015014
[25] Mansfield D.K. *et al* 2013 *Nucl. Fusion* **53** 7
[26] Ruzic D.N. *et al* 2011 *Nucl. Fusion* **51** 102002
[27] Ren J. *et al* 2014 *Phys. Scr.* **T159** 5
[28] Sun Z. *et al* 2013 *J. Nucl. Mater.* **438** S899
[29] Hu J.S. *et al* 2014 *Fusion Eng. Des.* **89** 2875
[30] Ren J. *et al* 2015 *Rev. Sci. Instrum.* **86** 023504
[31] Ding F. *et al* 2014 *J. Nucl. Mater.* **455** 710
[32] Zuo G.Z. *et al* 2013 *J. Nucl. Mater.* **438** S90
[33] Hu J.S. *et al* 2010 *Fusion Eng. Des.* **85** 930
[34] Zuo G.Z. *et al* 2014 *Fusion Eng. Des.* **89** 2886
[35] Apicella M.L. *et al* 2007 *J. Nucl. Mater.* **363–5** 1346
[36] Mirnov S.V. *et al* 2011 *Nucl. Fusion* **51** 073044